NASA/TM—2011–216463

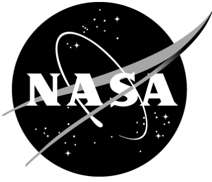

Microcoil Spring Interconnects for Ceramic Grid Array Integrated Circuits

S.M. Strickland, J.D. Hester, A.K. Gowan, R.K. Montgomery, and D.L. Geist
Marshall Space Flight Center, Marshall Space Flight Center, Alabama

J.F. Blanche and G.D. McGuire
Jacobs Engineering, Science and Technical Services Group
Marshall Space Flight Center, Marshall Space Flight Center, Alabama

T.S. Nash
Jacobs Engineering, Science and Technical Services Group/Integrated Concepts and Research, Marshall Space Flight Center, Marshall Space Flight Center, Alabama

March 2011

The NASA STI Program…in Profile

Since its founding, NASA has been dedicated to the advancement of aeronautics and space science. The NASA Scientific and Technical Information (STI) Program Office plays a key part in helping NASA maintain this important role.

The NASA STI Program Office is operated by Langley Research Center, the lead center for NASA's scientific and technical information. The NASA STI Program Office provides access to the NASA STI Database, the largest collection of aeronautical and space science STI in the world. The Program Office is also NASA's institutional mechanism for disseminating the results of its research and development activities. These results are published by NASA in the NASA STI Report Series, which includes the following report types:

- TECHNICAL PUBLICATION. Reports of completed research or a major significant phase of research that present the results of NASA programs and include extensive data or theoretical analysis. Includes compilations of significant scientific and technical data and information deemed to be of continuing reference value. NASA's counterpart of peer-reviewed formal professional papers but has less stringent limitations on manuscript length and extent of graphic presentations.

- TECHNICAL MEMORANDUM. Scientific and technical findings that are preliminary or of specialized interest, e.g., quick release reports, working papers, and bibliographies that contain minimal annotation. Does not contain extensive analysis.

- CONTRACTOR REPORT. Scientific and technical findings by NASA-sponsored contractors and grantees.

- CONFERENCE PUBLICATION. Collected papers from scientific and technical conferences, symposia, seminars, or other meetings sponsored or cosponsored by NASA.

- SPECIAL PUBLICATION. Scientific, technical, or historical information from NASA programs, projects, and mission, often concerned with subjects having substantial public interest.

- TECHNICAL TRANSLATION. English-language translations of foreign scientific and technical material pertinent to NASA's mission.

Specialized services that complement the STI Program Office's diverse offerings include creating custom thesauri, building customized databases, organizing and publishing research results…even providing videos.

For more information about the NASA STI Program Office, see the following:

- Access the NASA STI program home page at <http://www.sti.nasa.gov>

- E-mail your question via the Internet to <help@sti.nasa.gov>

- Fax your question to the NASA STI Help Desk at 443–757–5803

- Phone the NASA STI Help Desk at 443–757–5802

- Write to:
  NASA STI Help Desk
  NASA Center for AeroSpace Information
  7115 Standard Drive
  Hanover, MD 21076–1320

NASA/TM—2011–216463

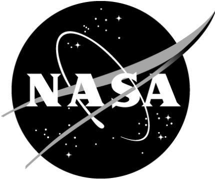

Microcoil Spring Interconnects for Ceramic Grid Array Integrated Circuits

S.M. Strickland, J.D. Hester, A.K. Gowan, R.K. Montgomery, and D.L. Geist
Marshall Space Flight Center, Marshall Space Flight Center, Alabama

J.F. Blanche and G.D. McGuire
Jacobs Engineering, Science and Technical Services Group
Marshall Space Flight Center, Marshall Space Flight Center, Alabama

T.S. Nash
Jacobs Engineering, Science and Technical Services Group/Integrated Concepts and Research, Marshall Space Flight Center, Marshall Space Flight Center, Alabama

National Aeronautics and
Space Administration

Marshall Space Flight Center • MSFC, Alabama 35812

March 2011

Acknowledgments

The authors would like to extend thanks to Mike Sampson, NASA Goddard Space Flight Center, Manager of the NASA Electronic Parts and Packaging Program, for his support of this effort. The authors would also like to recognize the following individuals for their technical support: Dr. Dhananjay Panchagade, Auburn University, for his support of the vibration testing, Ron Johnson, NASA Marshall Space Flight Center/ES43, for his support of fixture design/fabrication.

Available from:

NASA Center for AeroSpace Information
7115 Standard Drive
Hanover, MD 21076–1320
443–757–5802

This report is also available in electronic form at
<https://www2.sti.nasa.gov/login/wt/>

TABLE OF CONTENTS

1. INTRODUCTION 1

2. MICROCOIL DESIGN 3

3. TEST VEHICLE DESIGN AND EVALUATION 5

3.1 Interconnect First Attach to Ceramic Substrate 6
3.2 Board-Level Fabrication 7
3.3 Thermal Cycling 9
3.4 Vibration 11
3.5 Radio Frequency Simulation 15
3.6 Inductance Measurement 16

4. STRESS ANALYSIS 17

5. SUMMARY 19

6. FUTURE WORK 20

REFERENCES 21

LIST OF FIGURES

1. MCS design 3
2. Ceramic channel configuration 5
3. Test vehicle 6
4. Interconnect attachment fixture 7
5. MCS 4-mil stencil 8
6. Typical wire column 8
7. Polymer cored solder ball 8
8. Thermal cycling results 9
9. Failed MCS (MCS-2-U1-3) thermal cycling 10
10. Failed MCS (MCS-1-U1-4) thermal cycling 10
11. Vibration test vehicle 11
12. Wire staking 11
13. Fixture and shaker 12
14. Vibration failure locations 14
15. Column cracks 14
16. Column displacement 14
17. Simplified FEA model—(a) MCS and (b) column 17
18. Solder stress—MCS versus column 18
19. MCS fillet with 6-mil stencil 20

LIST OF TABLES

1. Test vehicle configuration 5

2. Vibration test levels.......... 13

3. Vibration failures 13

4. Power transferred—HFSS simulation—MCSs versus columns 15

5. Crosstalk (coupling)—HFSS simulation—MCSs versus columns 15

6. Maximum stress levels 18

LIST OF ACRONYMS AND SYMBOLS

Ag	silver
AU	Auburn University
Au	gold
CBGA	ceramic ball grid array
CCGA	ceramic column grid array
CTE	coefficient of thermal expansion
Cu	copper
DC	direct current
EEE	electrical, electronic, and electromechanical
HFSS	high-frequency structure simulator
I/O	input/output
MCS	microcoil spring
MSFC	Marshall Space Flight Center
Ni	nickel
PBGA	plastic ball grid array
Pb	lead
PCB	printed circuit board
Pd	palladium
RF	radio frequency
Sn	tin
TC	thermal cycling
W	tungsten

TECHNICAL MEMORANDUM

MICROCOIL SPRING INTERCONNECTS FOR CERAMIC GRID ARRAY INTEGRATED CIRCUITS

1. INTRODUCTION

Current aerospace avionic designs routinely use integrated circuits packaged in the area array format. Unfortunately, the area array package trades the compliance of ribbon leads for the quantity of noncompliant solder balls, which under thermal cyclic loading, severely limits the life of the solder joints.

One approach to overcome this limitation was to replace the noncompliant balls with slightly more compliant solder columns. Another approach was to package the silicon microcircuit on an organic substrate and plastic encapsulate it rather than put it on a ceramic substrate and hermetically seal it. The coefficient of thermal expansion (CTE) of a plastic ball grid array (PBGA) more closely matched the CTE of the printed circuit board (PCB) than the CTE of a ceramic ball grid array (CBGA). There are always tradeoffs to be made and the price initially paid for using a PBGA was that the plastic absorbed moisture and moisture could initiate corrosion and result in a failure rate that was unacceptable for high reliability space flight electronics. With time, the processes and materials have improved such that the moisture absorption is much lower but a plastic encapsulated microcircuit is still not a hermetically sealed part. Electrical, electronic, and electromechanical (EEE) parts personnel prefer ceramic column grid array (CCGA) packages for highest reliability critical applications.

Reliability of various configurations of flexible interconnects for ceramic area array packages are reported in the literature.[1–5] Variation in test methods and test vehicle configurations make it difficult to perform direct comparisons with a high confidence level. NASA Marshall Space Flight Center (MSFC) initiated a research project to test a variety of flexible interconnects while holding constant (as nearly as possible) the ceramic substrate design, PCB design, and test methods so that reliability could be fairly compared.

A long-term human presence in space without the benefit of resupply will require confidence levels not previously required. Due to this and existing reliability data on columns, MSFC started investigating other potential flexible interconnects to improve the thermal reliability of ceramic area array packages. Preliminary assembly experiments with springs of various configurations were conducted. As a result of these preliminary experiments, a microcoil spring (MCS) was chosen and introduced into the test program.

The MCSs provide ample flexibility to withstand the shear forces resulting from the CTE mismatch and are much more robust from a handling perspective than high lead columns. However, the MCSs do not have planarized end faces which makes attachment challenging.

2. MICROCOIL DESIGN

The MCS (fig. 1) is fabricated from a beryllium copper (Cu) wire 0.0034 in thick and is post plated with 100 µin of tin lead (Sn63Pb37). The springs are 0.020 in diameter by 0.050 in long with a 0.010 in pitch and two to three closed coils on each end.

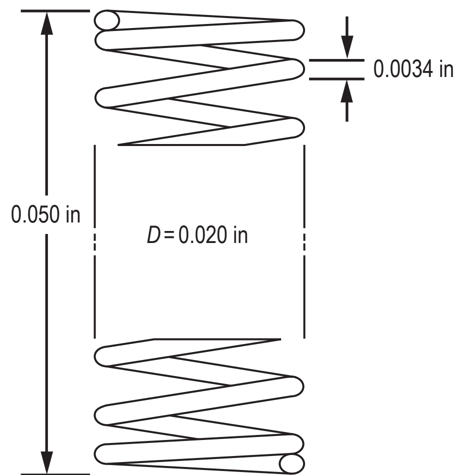

Figure 1. MCS design.

3. TEST VEHICLE DESIGN AND EVALUATION

The primary ceramic substrate and PCB were designed by MSFC's Parts, Packaging, and Fabrication Branch. The ceramic substrates are 21.5 mm × 21.5 mm × 1 mm. The substrates are daisy-chained, two layers and 1 mm pitch. Each substrate consists of four channels (fig. 2) which are made up of 100 daisy-chained interconnects. The current ceramic substrates were fabricated using a thick film technique with a minimum of three layers of silver (Ag)/palladium (Pd) paste to form metallization ≈0.001 in thick. The pad diameter has ranged from 0.025 to 0.030 in. Early in the study, 0.025 in was used due to the ball size chosen. Subsequently, the pad diameter was changed to 0.030 in to accommodate columns and MCSs. The same pad diameter is used on both the substrate and PCB. Early in the study a four-layer ceramic with tungsten (W)-nickel (Ni)-gold (Au) metallization was used, but it was abandoned due to cost. The interconnects tested with this metallization are noted in table 1.

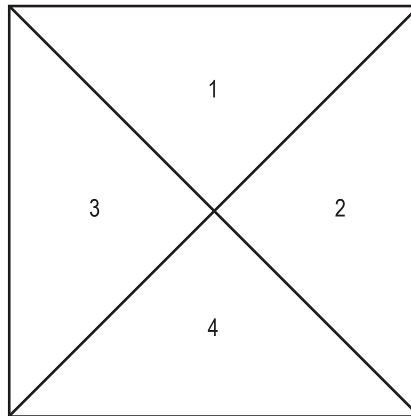

Figure 2. Ceramic channel configuration.

Table 1. Test vehicle configuration.

Test Vehicle*	No. of TV's	Ceramic Configuration	Solder Used for First Attach	Stencil Thickness/Aperture (PCB Attach)	Use
Initial MCS*	2	25 mil/Ag-Pd	Tin/lead	4 mil/100%	TC @ MSFC
95/5 CCGA	3	30 mil/Ag-Pd	Tin/lead	8 mil/100%	Vib @ AU then TC @ MSFC
85/15 CCGA*	1	25 mil/W-Ni-Au	Tin/lead	8 mil/100%	TC @ AU
90/10 CBGA*	2	25 mil/Ag-Pd	Tin/lead	4 mil/100%	TC @ MSFC
Polymer CBGA*	2	25 mil/Ag-Pd	Tin/lead	6 mil/100%	TC @ MSFC
Reworked MCS	3	30 mil/Ag-Pd	Tin/lead	6 mil/100% (1) and 4 mil/75% (2)	TC @ MSFC
MCS Vibration	1	30 mil/Ag-Pd	Tin/lead	4 mil/100%	Vib @ AU then TC @ MSFC

*All test vehicles with asterisks were fabricated using a 0.062-in, double-sided PCB with 0.025-in-diameter pads. The remainder were fabricated using a 0.093-in, double-sided PCB with 0.030-in pads.

Unless otherwise noted, the PCB (fig. 3) is four layers, two of which are ground planes for stiffness and is designed to accommodate eight parts. The overall thickness is 0.093 in.

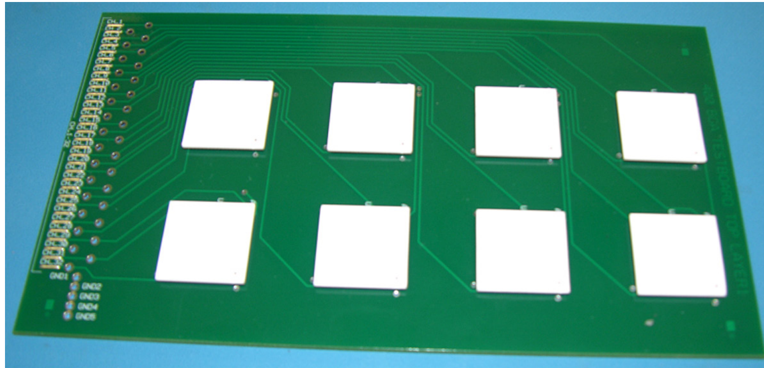

Figure 3. Test vehicle.

The following interconnects were included in the thermal cycling phase of the study:

- Sn5/Pb95 wire column (0.018×0.087 in).
- Sn15/Pb85 column (0.015×0.087 in).
- Polymer cored ball (650 µm).
- Sn10/Pb90 solder balls (0.025 in).
- MCS (0.020×0.050 in).

Vibration testing was conducted on test vehicles with Sn5/Pb95 wire columns and MCSs.

3.1 Interconnect First Attach to Ceramic Substrate

Except for the Sn15/Pb85 columns, all interconnects were attached by MSFC using a two-piece fixture (fig. 4) that holds a single ceramic substrate. Solder paste is deposited onto the ceramic substrate using an automatic stencil printer. After inspection, the substrate is loaded into a graphite fixture stage (bottom) and a graphite interconnect positioning fixture (top) is lowered onto the stage. The positioning fixture has apertures that match the pattern on the ceramic with the apertures sized for the interconnect diameter being attached. After the apertures are filled with interconnects, the whole fixture is loaded onto a pallet and reflowed in a vapor phase reflow oven. For ball interconnects, the interconnect positioning fixture (top) is removed prior to reflow which aids in ball to ceramic pad alignment.

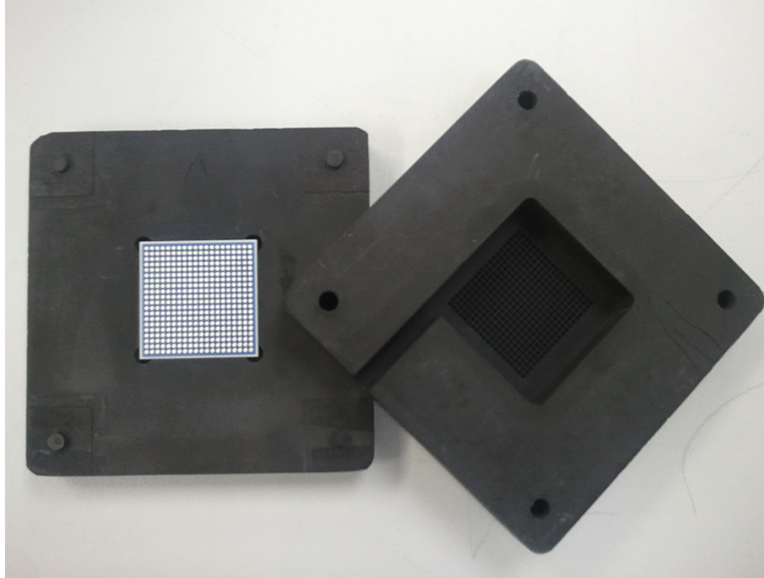

Figure 4. Interconnect attachment fixture.

For the MCS, the stencil thickness, stencil aperture size, and solder alloy were varied. The first thermal cycling test vehicles were fabricated using SnPb solder paste for attachment to both the ceramic substrate and the PCB. The stencil thickness was 0.004 in, resulting in the best thermal reliability to date. To improve yield, the solder paste for first attach (to ceramic) was changed to Sn-Ag-Cu (SAC305) to prevent its reflow and MCS movement during second attach. The stencil thickness has been optimized at 0.006 in for the MCS design currently being used. This results in the best fillets. Recently, a process step was added to remove MCS oxidation during first attach by using flux and a double reflow process which has allowed a return to SnPb paste without a decrease in yield. Thermal cycling for test vehicles fabricated using the double-pass reflow process and a 0.006-in-thick stencil is ongoing and results are not presented herein.

3.2 Board-Level Fabrication

Solder paste was deposited using an automatic stencil printer. Part placement was achieved using a semi-automatic, split-vision placement machine. Reflow except for rework was conducted in a vapor phase reflow oven. Endoscopic and x-ray inspections were performed prior to initiation of environmental testing. A typical MCS from the first thermal cycling test vehicle is presented in figure 5. Notice the lack of side fillets.

A typical wire column (Sn5/Pb95) is shown in figure 6. An 8-mil-thick stencil was used to attach the Sn5/Pb95 columns to both the ceramic and the PCB.

A typical polymer cored solder ball is shown in figure 7. The ball is 650 μm and has a Sn-Ag over Cu finish. A 6-mil-thick stencil was used to attach the polymer cored solder balls to both the ceramic and the PCB.

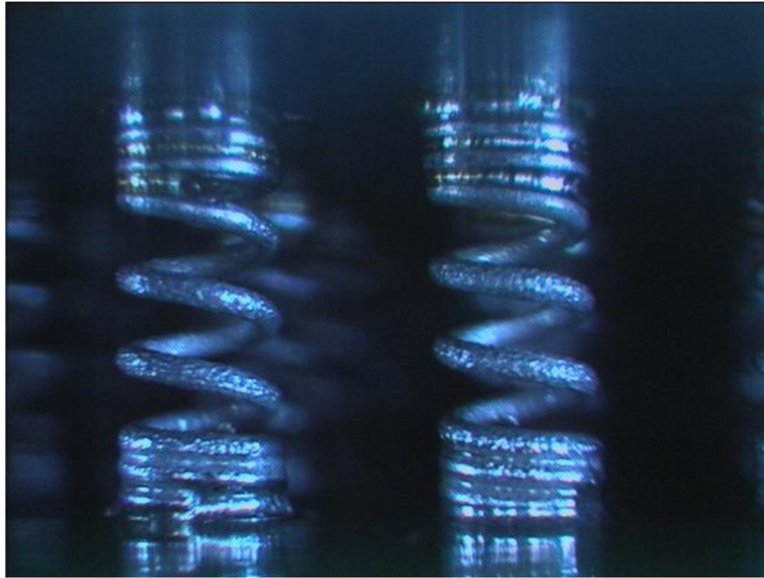

Figure 5. MCS 4-mil stencil.

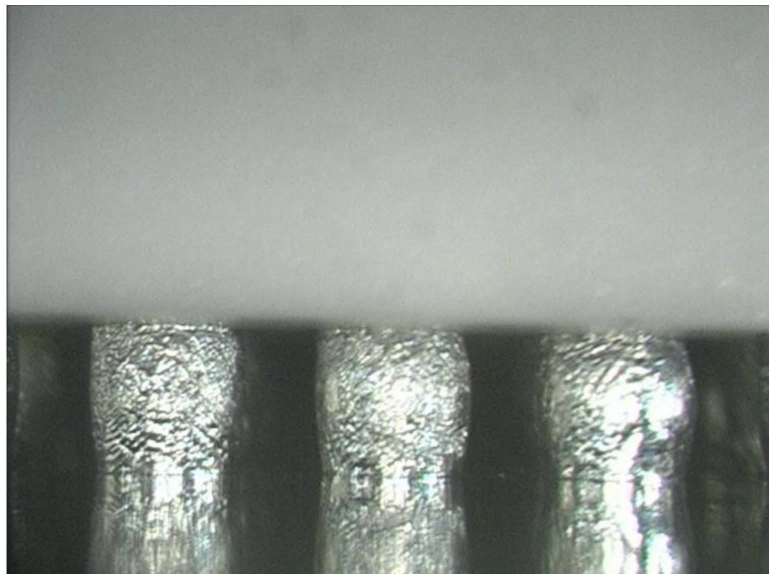

Figure 6. Typical wire column.

Figure 7. Polymer cored solder ball.

The overall test vehicle configuration is presented in table 1 along with the environmental tests performed on each unit.

3.3 Thermal Cycling

Thermal cycling was conducted at MSFC and at Auburn University (AU). The range was –55 to 125 °C with 15-min dwells at the extremes. Auburn University conducted the thermal cycling of the 85/15 CCGA test vehicles. MSFC performed the thermal cycling of the remainder of the test vehicles.

The AU tests were monitored using a data logger. The failure criteria used was a 50% increase in resistance for 10 consecutive thermal cycles. The AU testing consisted of 400 interconnects per channel and one 85/15 CCGA test board with five parts. Testing was conducted in a thermal cycling chamber.

The MSFC tests were monitored using an event detector. The failure criteria were per IPC-9701A, 4.3.3.3, with a 1,000 Ω threshold. Testing was conducted in a thermal forcing unit with a custom enclosure; ≈19 cycles per day were obtained.

A composite Weibull is shown in figure 8. The initial MCS (MCS on 25-mil pad) significantly outperformed 85/15 CCGAs and 95/5 CCGAs. The initial MCS test vehicles had many individual springs that were misaligned to the PCB pads by as much as 50%. The first recordable failure (other than one infant mortality at 400 cycles) occurred at 4,760 cycles. For space flight systems, first failure is considered a more important factor than characteristic life.

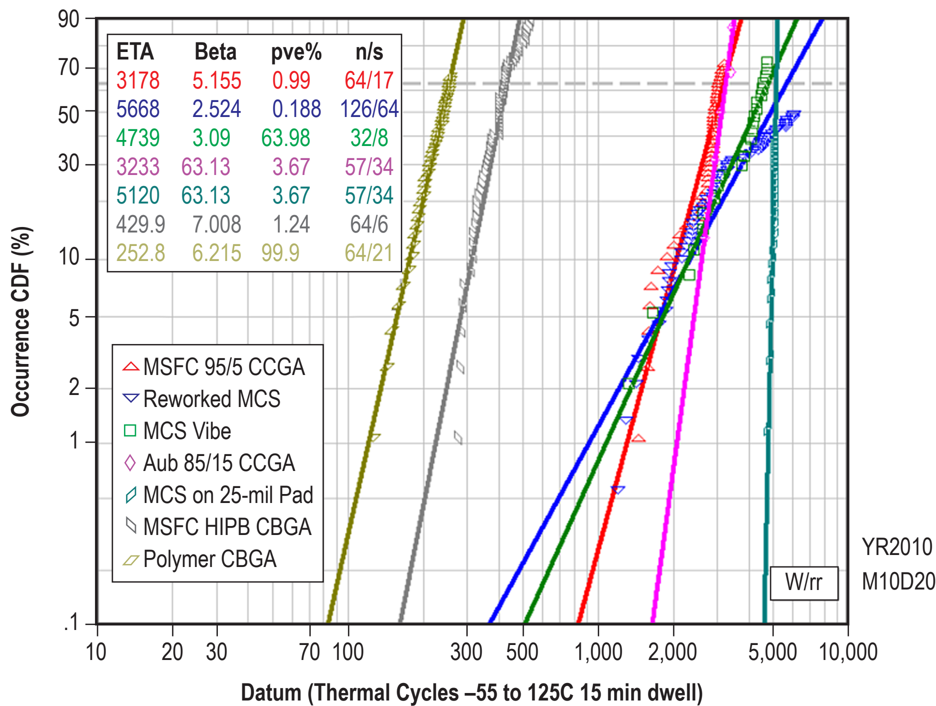

Figure 8. Thermal cycling results.

Metallographic analysis and endoscopy of failed MCSs (figs. 9 and 10) and 95/5 columns were performed to verify failure mode. All MCS failures observed were in the solder joint interface with the ceramic pad. The failures appear to have begun parallel to the interface which is expected, but as the failure propagated, a perpendicular crack developed in several of the microsections observed. Metallographic analysis was also used to verify that the Ag-Pd pad on the ceramic was not being leached into the solder joint during multiple reflows. No evidence of pad failure or significant leaching was found.

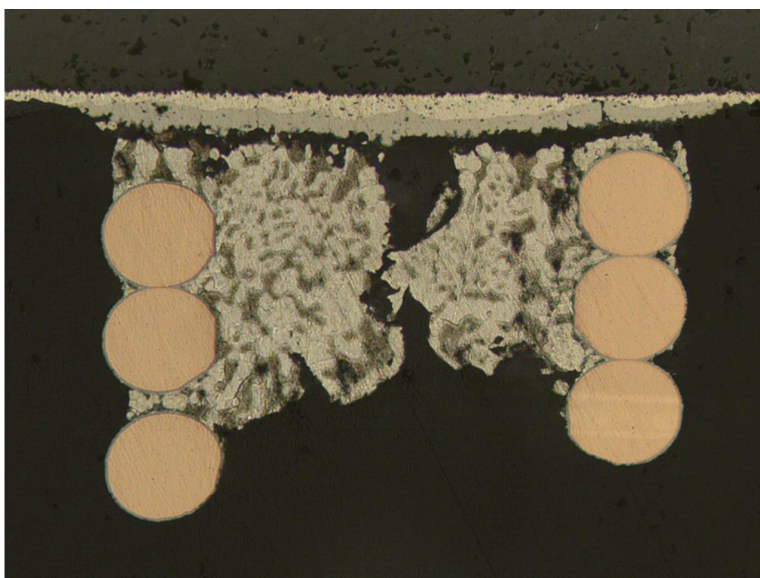

Figure 9. Failed MCS (MCS-2-U1-3) thermal cycling.

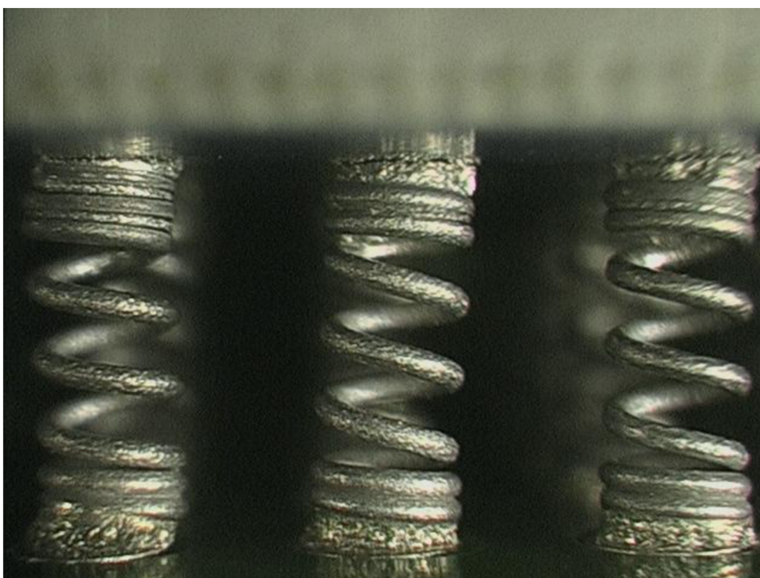

Figure 10. Failed MCS (MCS-1-U1-4) thermal cycling.

3.4 Vibration

Vibration testing was conducted at AU. The test vehicles used the same PCB and ceramic parts. The only difference from the thermal cycling test vehicles is that an aluminum mass was attached to each ceramic to simulate the mass of a comparably sized active ceramic package (fig. 11). One 95/5 CCGA and one MCS test vehicle were vibration tested.

Each test vehicle was hard wired to a shielded cable that attached to an event detector system. An event was recorded when the channel resistance exceeded 1,000 Ω, which in each case, constituted a failure since these resistance changes were hard and did not show intermittency. The wires were staked to the back side of the board (fig. 12).

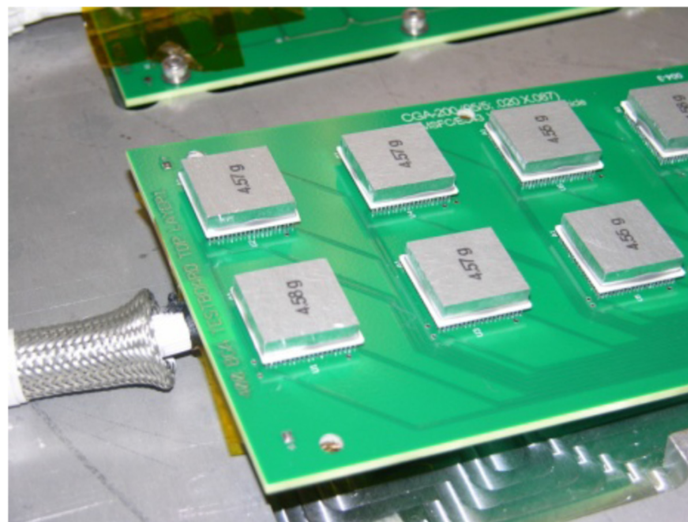

Figure 11. Vibration test vehicle.

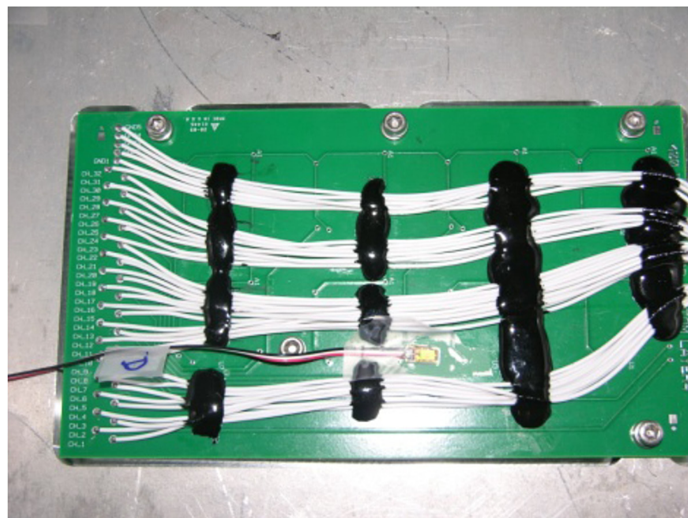

Figure 12. Wire staking.

The test vehicles mounted to the vibration fixture and the shaker table are shown in figure 13.

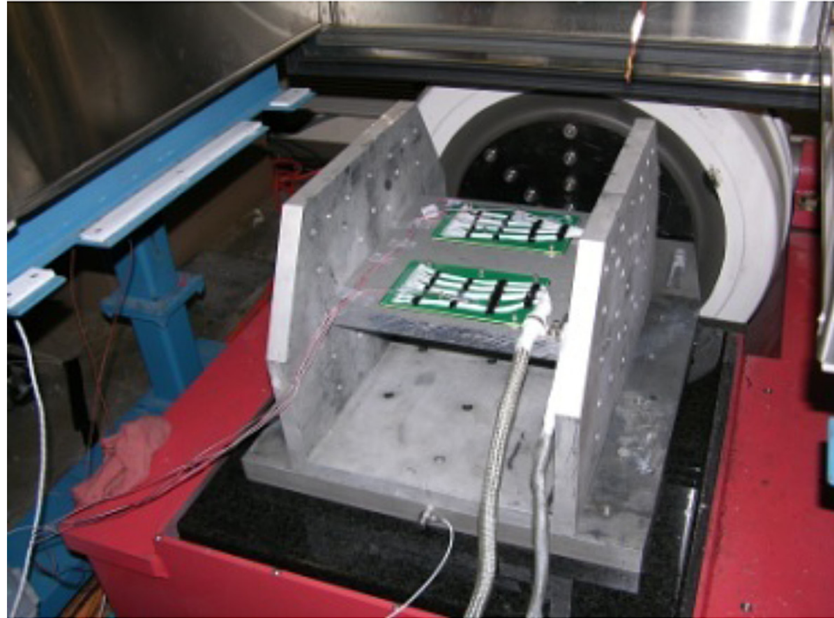

Figure 13. Fixture and shaker.

Prior to performing the random vibration test a resonance search sine sweep was performed with the boards mounted in the *x* axis at a sweep range 5–2,000–5 Hz, sweep rate: two octaves per minute, amplitude 0.25 g.

The *z* axis is perpendicular to the surface of the unit under test. The *x* axis is defined as the shortest board dimension (4 in). Random vibration testing was performed at three different levels for 10 min at each level in the *x* axis and the *z* axis, for a total test time of 1 hr. The random vibration levels are presented in table 2.

The testing sequence was 0.25 g sine sweep, 5g*x*, 5g*z*, 8g*z*, 8g*x*, 10g*x*, and 10g*z*. There was a system natural frequency at ≈420 Hz and another at 900 Hz. The MCSs were recorded as channels 1–32 and the 95/5 columns as channels 33–64. Throughout the test there were no failures of the MCSs. There were 10 failures of the 95/5 columns. The failure data are shown in table 3. The location of the failed circuits on the column grid array test board is shown in figure 14. The failures were resistance failures only. No parts were shaken off of the boards.

Table 2. Vibration test levels.

<table>
<tr><th colspan="2">Level I</th></tr>
<tr><td>20 Hz @
20–50 Hz @
50–1,000 Hz @
1,000–2000 Hz @
2,000 Hz @</td><td>0.0025 g^2/Hz
6 dB/oct
0.01675 g^2/Hz
–6 dB/oct
0.005 g^2/Hz</td></tr>
<tr><td colspan="2">Composite = 5 gm</td></tr>
<tr><th colspan="2">Level II</th></tr>
<tr><td>20 Hz @
20–50 Hz @
50–1,000 Hz @
1,000–2,000 Hz @
2,000 Hz @</td><td>0.00698 g^2/Hz
6 dB/oct
0.0438 g^2/Hz
–6 dB/oct
0.0109 g^2/Hz</td></tr>
<tr><td colspan="2">Composite = 8 gm</td></tr>
<tr><th colspan="2">Level III</th></tr>
<tr><td>20 Hz @
20–50 Hz @
50–1000 Hz @
1,000–2,000 Hz @
2,000 Hz @</td><td>0.01 g^2/Hz
6 dB/oct
0.067 g^2/Hz
–6 dB/oct
0.02 g^2/Hz</td></tr>
<tr><td colspan="2">Composite = 10 gm</td></tr>
</table>

Table 3. Vibration failures.

g Level	Axis	Failed Channel	Time Into Run (min)	Total Vibration Time to Failure (min)
5	x	–	–	–
5	z	59	10	20
8	z	61	4	24
8	z	62	7	27
8	x	58	6	36
10	x	57	6	46
10	z	44	3	53
10	z	33	5	55
10	z	41	7	57
10	z	42	7	57
10	z	36	8	58

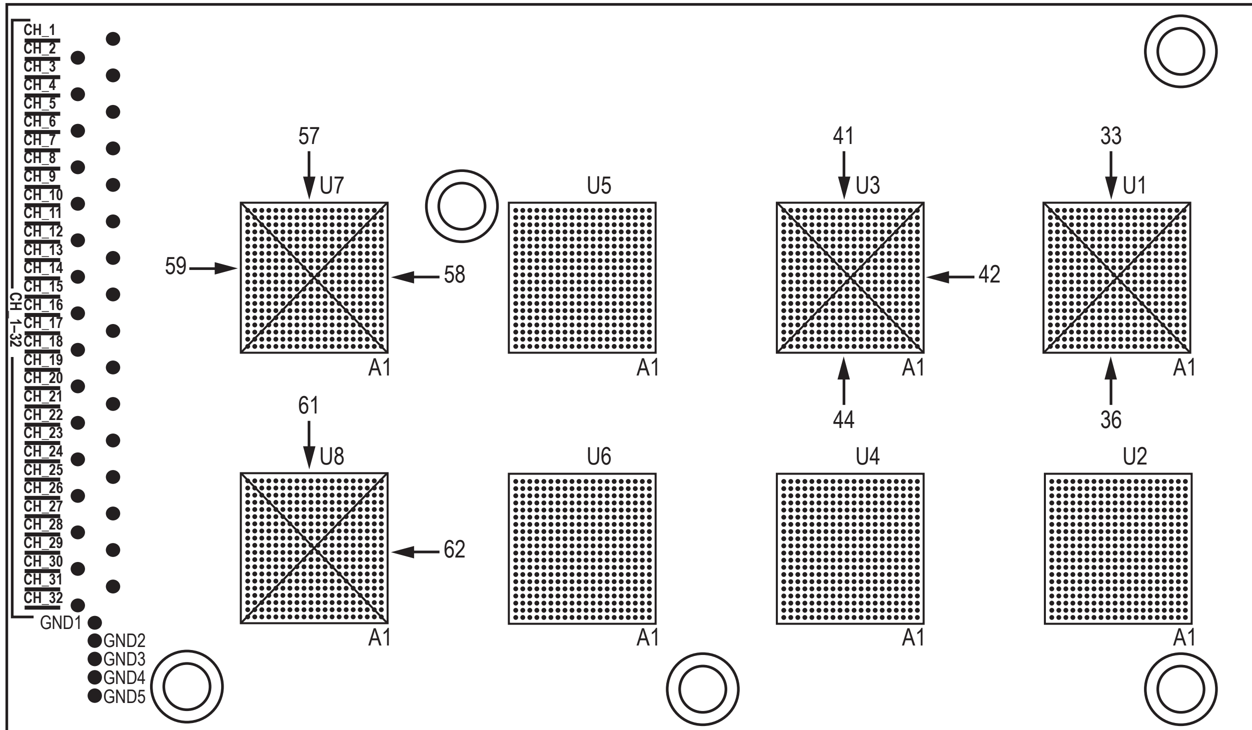

Figure 14. Vibration failure locations.

The failures were investigated by endoscopy, x-ray, and destructive physical analysis. The outer rows of columns of failed channels were subjected to endoscopic visual inspection. Cracks were observed in the columns generally at the point where the 63/37 solder fillet joined the column. Figure 15 shows examples of cracks in both the upper and lower fillets. Figure 16 shows the most extreme failure observed.

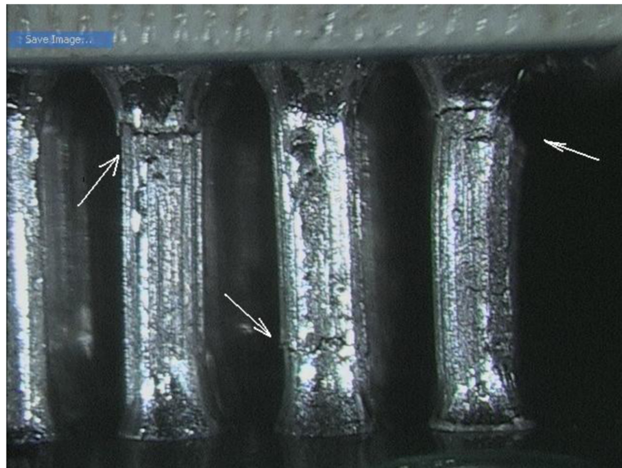

Figure 15. Column cracks.

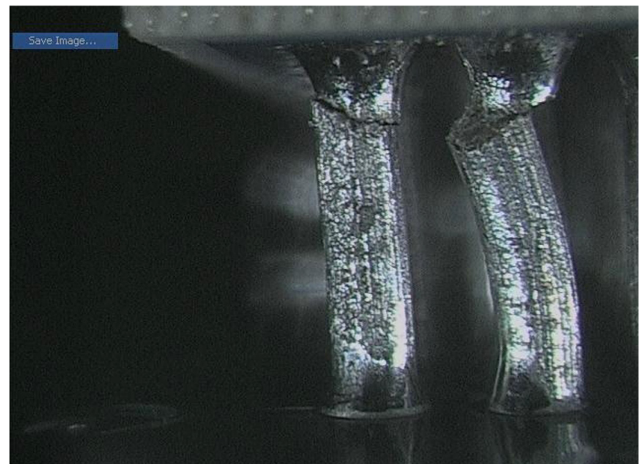

Figure 16. Column displacement.

3.5 Radio Frequency Simulation

Radio frequency simulations were run on the MCS and the column configurations. The simulation was performed from the kilohertz range up to 10 GHz. The insertion loss, the coupling (crosstalk), and the effective inductance of each configuration was simulated and compared. The simulations were done with a high-frequency structure simulator (HFSS) at MSFC in the Data and Radio Frequency Systems Branch of the Space Systems Department.

Table 4 compares the insertion loss for MCSs and columns over a frequency range of 500 MHz to 5 GHz. The insertion loss shows how much power is transferred from one end of the column or MCS to the other. The insertion loss of the MCS configuration is a little worse than the column configuration. The insertion loss of each configuration is similar at the lower frequencies. As the frequency increases, the insertion loss of the MCS increases slightly faster than the column. The difference in performance decreases as the configurations are used at lower frequencies.

Table 4. Power transferred—HFSS simulation—MCSs versus columns.

Frequency	MCS (%)	Column (%)
500 MHz	98.3	98.9
1 GHz	96.4	97.9
2 GHz	89	92.5
3 GHz	79.1	85.0
4 GHz	69.1	77.0
5 GHz	59.8	69.3

Table 5 compares coupling (crosstalk) of MCSs and columns. The coupling shows how much power is transferred from one column to an adjacent column. The coupling of the MCS versus the column is slightly better at the lower frequencies but then becomes much better at the higher frequencies. The worst coupling of the MCS configuration was about –22.9 dB (0.52% power transfer), which occurred at 4 GHz. At this frequency, the coupling of the column configuration was –13 dB (5% power transfer). However, the coupling of the MCS improves slightly as the frequency increases whereas the coupling of the column degrades. The worst coupling of the column configuration was about –10 dB (10% power transfer), which occurred at 9.9 GHz.

Table 5. Crosstalk (coupling)—HFSS simulation—MCSs versus columns.

Frequency	MCS (%)	Column (%)
500 MHz	0.086	1.19
1 GHz	0.17	0.4
2 GHz	0.59	1.5
3 GHz	1.06	2.9
4 GHz	1.4	4.4
5 GHz	1.7	5.8

The inductance of the MCS and the column configurations was calculated over the frequency range of the simulation (500 MHz to 10 GHz). The inductance of the MCS was 2.7 nH, and the inductance of the column was 2.2 nH.

3.6 Inductance Measurement

The inductance of one test vehicle channel which is comprised of 100 interconnects was determined using a frequency analyzer capable of measurements up to 2.2 MHz. This frequency range was sufficient to show the inductive component of the interconnects but it was not sufficient to show parasitic capacitances which often show up in higher frequency ranges. The data for each test vehicle includes the inductive contribution due to the test leads connecting the test units and the instrument. The contribution of the test leads can be subtracted from the data. What cannot be removed is the resistance and inductance associated with the interconnections between 100 individual interconnects. It may be assumed that they are small but a more precise evaluation of the interconnects needs to be performed using an inductance/capacitance/resistance bridge or frequency response analyzer and a test fixture capable of holding individual interconnects.

The MCS DC resistance component was measured at ≈3 Ω and the inductive component was measured at ≈484 nH (after the inductance of the test leads is subtracted). Since there are 100 interconnects in series, the per unit resistance and inductance is calculated as follows:

- Per unit DC resistance = 3 Ω/100 = 0.03 Ω.
- Per unit inductance = 484 nH/100 = 4.84 nH.

The column DC resistance measured at ≈0.9 Ω and an inductive component was measured at ≈591 nH (after the inductance of the test leads is subtracted). Since there are 100 interconnects in series, the per unit resistance and inductance is calculated as follows:

- Per unit DC resistance = 0.9 Ω/100 = 0.009 Ω
- Per unit inductance = 591 nH/100 = 5.91 nH.

4. STRESS ANALYSIS

A simplified finite element model of an MCS and a column was created (see fig. 17) and a stress analysis was performed to illustrate the stress on the two interconnects for given deflections (see fig. 18).

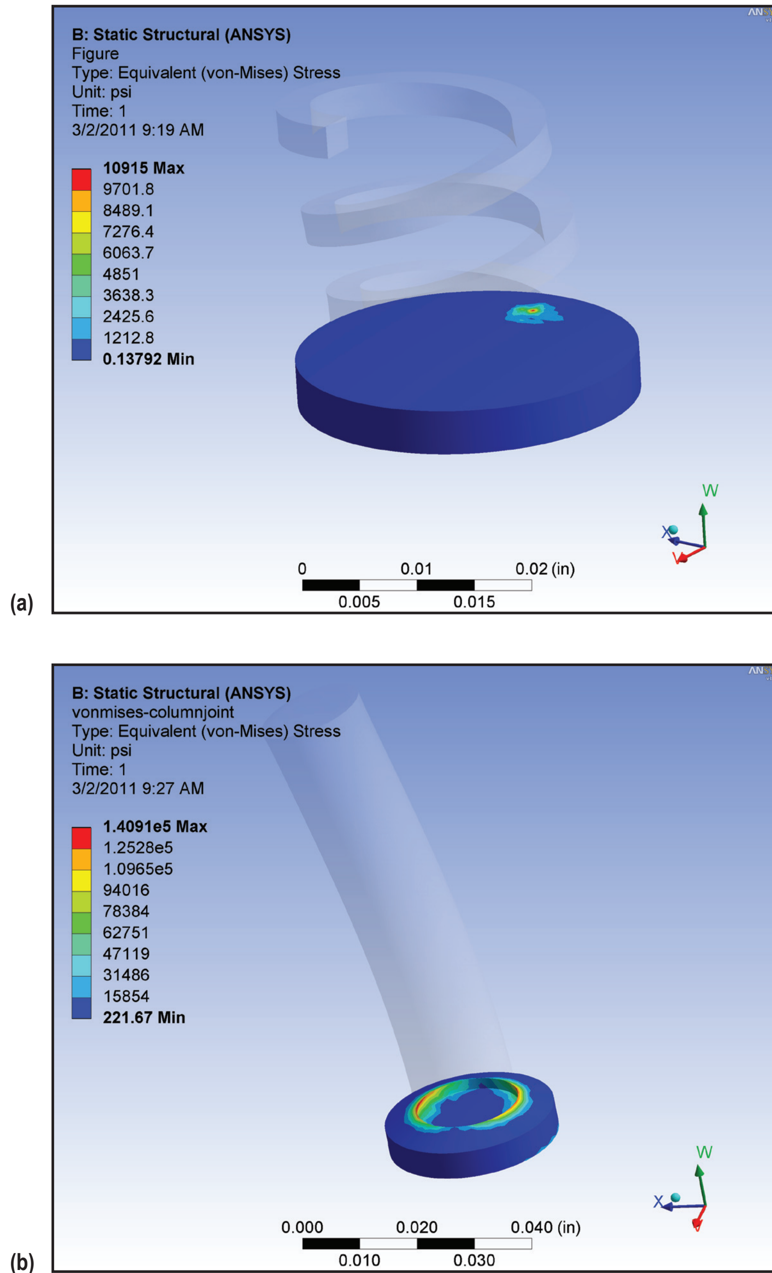

Figure 17. Simplified FEA model—(a) MCS and (b) column.

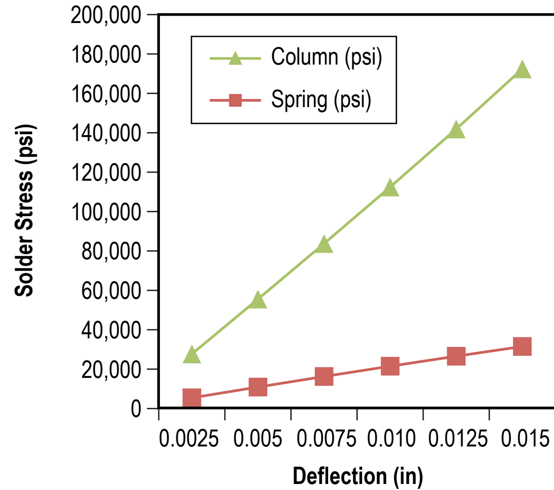

Figure 18. Solder stress—MCS versus column.

A preliminary assessment was conducted to determine the Von Mises stress in the solder joints associated with the MCS versus column configuration. This was a static analysis conducted using the finite element analysis software ANSYS Workbench. For the analysis, a deflection was assigned beginning with 0.0025 in and progressing up to 0.015 in in 0.0025-in increments. The maximum stress levels determined from this deflection are shown in table 6 regarding the solder joints for both the MCS and column configurations. These results are theoretical and have not been verified by testing.

Table 6. Maximum stress levels.

Deflection (in)	MCS (psi)	Column (psi)
0.0025	5,455	22,248
0.0050	10,915	44,656
0.0075	16,282	67,477
0.0100	21,499	90,962
0.0125	26,571	115,360
0.0150	31,525	140,915

5. SUMMARY

Thermal cycling and vibration testing have shown MCS interconnects to be significantly more reliable than solder columns. Also, MCS interconnects are less prone to handling damage than solder columns. While attachment of MCS parts to PCBs is more challenging than columns, they do not require shearing to obtain acceptable coplanarity.

Initial thermal cycling yielded better results than subsequent testing. The samples tested since the initial MCS reported herein were fabricated using a process that resulted in higher yields but lower reliability. The current process is very similar to the initial process except for addition of a deoxidizing step.

MCSs are expected to outperform columns in a mechanical shock environment based on deflection analysis and preliminary shock testing.

With further refinement of the attach process, it is anticipated that CGAs populated with MCSs can achieve >5,000 thermal cycles prior to first failure without the need for mechanical corner support.

MCSs can be manufactured with overall diameter as small as 0.006 in using conventional microcoiling technology. It is possible to use MCSs on column grid arrays down to 0.65-mm pitch.

An important item to note is that the MCS design has not been optimized for reliablility; only the part/PCB fabrication parameters have been varied to improve second attach. With a change in MCS parameters (i.e., number of active/closed coils, overall length), reliability could be further improved. Of course, physical changes to the MCS must be traded with changes in inductance, capacitance, crosstalk, and insertion loss.

6. FUTURE WORK

Testing of process improvements to remove oxidation and to improve the MCS to ceramic/PCB fillets is ongoing. Fillets that result from depositing solder with a 0.006-in-thick stencil are shown in figure 19. The fillets are much improved, however, the open coils of the MCS are more restrained.

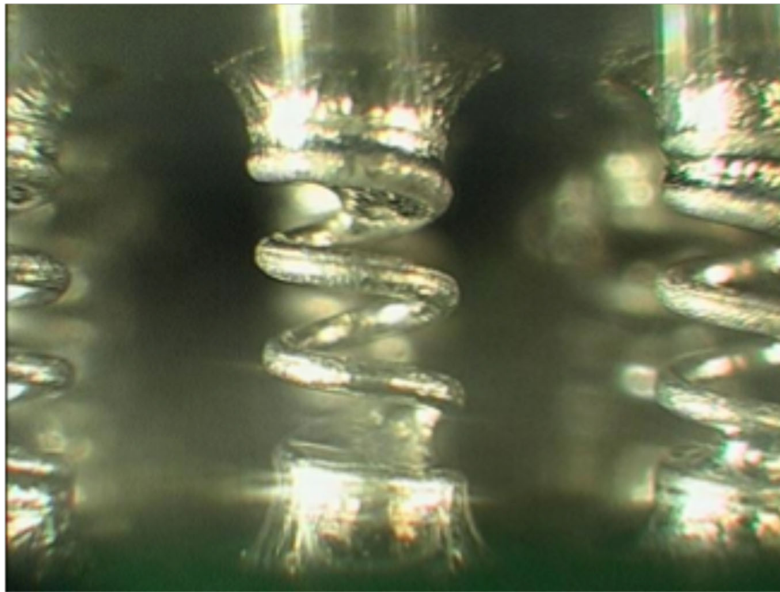

Figure 19. MCS fillet with 6-mil stencil.

An extensive mechanical shock test program is underway and is currently in the fabrication phase. Testing will be conducted by AU and will include MCSs and 95/5 columns. Completion of this study is needed to provide confidence for MCSs use in applications with high g liftoff environments.

Implementation of MCSs in a digital signal processor board has begun and is currently in the procurement phase. After fabrication completion, functional testing of the design will be conducted to judge the effects on circuit function and rise time in particular.

Testing of the current MCS design on a higher input/output (I/O) daisy-chained ceramic substrate is planned within the next year. The substrate will consist of 1,152 I/O. Also, design of a smaller diameter MCS is in process for testing on a daisy-chained ceramic substrate with 0.80-mm pitch.

A cast Sn10/Pb90 column (0.020 in diameter) is being added to the test program this year.

REFERENCES

1. Kuang, R.; and Zhao, L.: "Thermal Cycling Test Report for Ceramic Column Grid Array Packages—CCGA," Actel White Paper, 26 pp., Publication Year Unknown.

2. "Solder Column Qualification for Ceramic Column Grid Array (CCGA) White Paper," Aeroflex, 2008.

3. Lau, J.: "Reliability Testing and Data Analysis of an 1657CCGA (Ceramic Column Grid Array) Package with Lead-Free Solder Paste on Lead-Free PCBs (Printed Circuit Boards)," *Proceedings*, *54th IEEE Electronic Components and Technology Conference*, Vol. 1, pp. 718–725, 10.1109/ECTC.2004.1319417, 2004.

4. Perkins, A.; and Sitaraman, S.: "Vibration-Induced Solder Joint Failure of a Ceramic Column Grid Array (CCGA) Package," *Proceedings*, *54th IEEE Electronic Components and Technology Conference*, Vol. 2, pp. 1271–1278, 10.1109/ECTC.2004.1320277, 2004.

5. Ghaffarian, R.: "Thermal Cycle Reliability and Failure Mechanisms of CCGA and PBGA Assemblies With and Without Corner Staking," *IEEE Transactions on Components and Packaging Technologies*, Vol. 32, Issue 2, pp. 285–296, 10.1109/TCAPT.2008.921626, 2008.

REPORT DOCUMENTATION PAGE

Form Approved OMB No. 0704-0188

The public reporting burden for this collection of information is estimated to average 1 hour per response, including the time for reviewing instructions, searching existing data sources, gathering and maintaining the data needed, and completing and reviewing the collection of information. Send comments regarding this burden estimate or any other aspect of this collection of information, including suggestions for reducing this burden, to Department of Defense, Washington Headquarters Services, Directorate for Information Operation and Reports (0704-0188), 1215 Jefferson Davis Highway, Suite 1204, Arlington, VA 22202-4302. Respondents should be aware that notwithstanding any other provision of law, no person shall be subject to any penalty for failing to comply with a collection of information if it does not display a currently valid OMB control number.

PLEASE DO NOT RETURN YOUR FORM TO THE ABOVE ADDRESS.

1. REPORT DATE *(DD-MM-YYYY)*	2. REPORT TYPE	3. DATES COVERED *(From - To)*
01–03–2011	Technical Memorandum	

4. TITLE AND SUBTITLE

Microcoil Spring Interconnects for Ceramic Grid Array Integrated Circuits

5a. CONTRACT NUMBER

5b. GRANT NUMBER

5c. PROGRAM ELEMENT NUMBER

6. AUTHOR(S)

S.M. Strickland, J.D. Hester, A.K. Gowan, R.K. Montgomery, D.L. Geist, J.F. Blanche,* G.D. McGuire,* and T.S. Nash**

5d. PROJECT NUMBER

5e. TASK NUMBER

5f. WORK UNIT NUMBER

7. PERFORMING ORGANIZATION NAME(S) AND ADDRESS(ES)

George C. Marshall Space Flight Center
Marshall Space Flight Center, AL 35812

8. PERFORMING ORGANIZATION REPORT NUMBER

M–1312

9. SPONSORING/MONITORING AGENCY NAME(S) AND ADDRESS(ES)

National Aeronautics and Space Administration
Washington, DC 20546–0001

10. SPONSORING/MONITOR'S ACRONYM(S)

NASA

11. SPONSORING/MONITORING REPORT NUMBER

NASA/TM—2011–216463

12. DISTRIBUTION/AVAILABILITY STATEMENT

Unclassified-Unlimited
Subject Category 19
Availability: NASA CASI (443–757–5802)

13. SUPPLEMENTARY NOTES

Prepared by the Space Systems Department, Engineering Directorate
*Jacobs Engineering, Science and Technical Services Group
**Jacobs Engineering, Science and Technical Services Group/Integrated Concepts and Research Corp.

14. ABSTRACT

As integrated circuit miniaturization trends continue, they drive the need for smaller higher input/output (I/O) packages. Hermetically sealed ceramic area array parts are the package of choice by the space community for high reliability space flight electronic hardware. Unfortunately, the coefficient of thermal expansion mismatch between the ceramic area array package and the epoxy glass printed wiring board limits the life of the interconnecting solder joint. This work presents the results of an investigation by Marshall Space Flight Center into a method to increase the life of this second level interconnection by the use of compliant microcoil springs. The design of the spring and its attachment process are presented along with thermal cycling results of microcoil springs (MCS) compared with state-of-the-art ball and column interconnections. Vibration testing has been conducted on MCS and high lead column parts. Radio frequency simulation and measurements have been made and the MCS has been modeled and a stress analysis performed. Thermal cycling and vibration testing have shown MCS interconnects to be significantly more reliable than solder columns. Also, MCS interconnects are less prone to handling damage than solder columns. Future work that includes shock testing, incorporation into a digital signal processor board, and process evaluation of expansion from a 400 I/O device to a device with over 1,100 I/O is identified.

15. SUBJECT TERMS

electrical interconnects, ceramic grid array packages, microcoil springs, solder columns, electronic packaging, electronic fabrication

16. SECURITY CLASSIFICATION OF: a. REPORT	b. ABSTRACT	c. THIS PAGE	17. LIMITATION OF ABSTRACT	18. NUMBER OF PAGES
U	U	U	UU	28

19a. NAME OF RESPONSIBLE PERSON

STI Help Desk at email: help@sti.nasa.gov

19b. TELEPHONE NUMBER ***(Include area code)***

STI Help Desk at: 443–757–5802

National Aeronautics and
Space Administration
IS20
George C. Marshall Space Flight Center
Marshall Space Flight Center, Alabama
35812